

Northumbria Research Link

Citation: Atherton, Shaun, Polak, Daniel, Hamlett, Christopher, Shirtcliffe, Neil, McHale, Glen, Ahn, Sujung, Doerr, Stefan, Bryant, Robert and Newton, Michael (2016) Drop impact behaviour on alternately hydrophobic and hydrophilic layered bead packs. *Chemical Engineering Research and Design*, 110. pp. 200-208. ISSN 0263-8762

Published by: Elsevier

URL: <http://dx.doi.org/10.1016/j.cherd.2016.02.011>
<<http://dx.doi.org/10.1016/j.cherd.2016.02.011>>

This version was downloaded from Northumbria Research Link:
<http://nrl.northumbria.ac.uk/id/eprint/26381/>

Northumbria University has developed Northumbria Research Link (NRL) to enable users to access the University's research output. Copyright © and moral rights for items on NRL are retained by the individual author(s) and/or other copyright owners. Single copies of full items can be reproduced, displayed or performed, and given to third parties in any format or medium for personal research or study, educational, or not-for-profit purposes without prior permission or charge, provided the authors, title and full bibliographic details are given, as well as a hyperlink and/or URL to the original metadata page. The content must not be changed in any way. Full items must not be sold commercially in any format or medium without formal permission of the copyright holder. The full policy is available online: <http://nrl.northumbria.ac.uk/policies.html>

This document may differ from the final, published version of the research and has been made available online in accordance with publisher policies. To read and/or cite from the published version of the research, please visit the publisher's website (a subscription may be required.)



**Northumbria
University**
NEWCASTLE



University**Library**



Contents lists available at ScienceDirect

Chemical Engineering Research and Design

IChemE ADVANCING CHEMICAL ENGINEERING WORLDWIDE

journal homepage: www.elsevier.com/locate/cherd

Drop impact behaviour on alternately hydrophobic and hydrophilic layered bead packs

Shaun Atherton^{a,*}, Daniel Polak^a, Christopher A.E. Hamlett^a,
Neil J. Shirtcliffe^b, Glen McHale^c, Sujung Ahn^d, Stefan H. Doerr^d,
Robert Bryant^d, Michael I. Newton^a

^a School of Science and Technology, Nottingham Trent University, Clifton Lane, Nottingham NG11 8NS, UK^b Department of Technology and Bionics, Hochschule Rhein-Waal, Landwehr 4, Kleve 47533, Germany^c Faculty of Engineering & Environment, Northumbria University, Ellison Place, Newcastle upon Tyne NE1 8ST, UK^d College of Science, Swansea University, Singleton Park, Swansea SA2 8PP, UK

ARTICLE INFO

Article history:

Received 21 August 2015

Received in revised form 11 January

2016

Accepted 9 February 2016

Available online xxx

Keywords:

Hydrophobicity

Hydrophilicity

Drop impact

Water repellent soil

Soil science

Liquid marbles

ABSTRACT

A high level of water repellency in soils has an impact on soil hydrology, plant growth and soil erosion. Studies have been performed previously on model soils; consisting of close packed layers of glass spheres (140–400 µm in diameter), to mimic the behaviour of rain water on water repellent soils. In this study measurements were performed on multi-layered bead packs, to assess the interaction of water drops impacting layers consisting of different hydrophobic and hydrophilic layers. A high speed video camera was used to record the impact behaviour of water droplets on the bead packs focussing on the spreading of the droplet and the subsequent rebound behaviour of the droplet. Observations were made from the videos of the liquid marble effect on the droplet, whereby hydrophobic particles form a coating around the droplet, and how it differed depending on the arrangement of hydrophobic and hydrophilic layers within the bead pack. The droplet release height was varied in order to establish a relationship between impact velocity and the degree to which liquid marbling occurs, with higher impact speeds leading to a greater degree of liquid marbling. Measurements were also made to find the transition speeds between the three rebound conditions; rebound, pinning and fragmentation, showing an overall decrease in pinning velocity as the bead size increased.

© 2016 The Institution of Chemical Engineers. Published by Elsevier B.V. All rights reserved.

1. Introduction

Hydrophobicity is normally defined by the size of the contact angle of a water droplet on a surface. A more water repellent surface will result in a droplet exhibiting a high contact angle when in contact with the surface (Shirtcliffe et al., 2010). In the case of a rough surface, such as soil, water will typically take on one of two different wetting states, Fig. 1. The Cassie–Baxter state is where the water cannot infiltrate the gaps between the surface roughness, leaving a layer of trapped air below the liquid (Cassie and Baxter, 1944). In the Wenzel state the

liquid infiltrates the gaps and increases the surface contact area (Wenzel, 1936). While chemically induced hydrophobicity has a contact angle upper limit of ≈120°, as shown by fluoropolymers such as polytetrafluoroethylene (PTFE) (Zisman, 1964); complex surface topography can increase the contact angle even further, with super-hydrophobic materials having a contact angle of over 160°.

Typically the minerals found naturally in soils, e.g. silica in sandy soils, display hydrophilic properties. However, with the addition of contaminants, such as oils, other naturally occurring organic matter, the soil particles can become hydrophobic

* Corresponding author. Tel.: +44 01158488391.

E-mail address: shaun.atherton02@ntu.ac.uk (S. Atherton).

<http://dx.doi.org/10.1016/j.cherd.2016.02.011>

0263-8762/© 2016 The Institution of Chemical Engineers. Published by Elsevier B.V. All rights reserved.

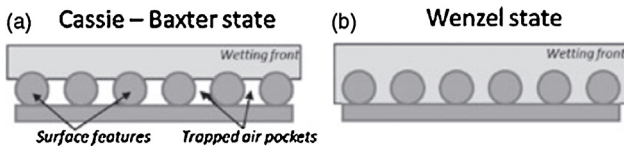


Fig. 1 – Diagram showing the (a) Cassie–Baxter and (b) Wenzel states of wetting. (Hamlett et al., 2013).

(Doerr et al., 2000; Ellerbrock et al., 2005; Atanassova and Doerr, 2010). Due to their granular nature, soil particles will form a matrix with a hierarchical structure with individual grains providing a rough topography; and each individual particle also possessing a rough surface. Combining this rough surface structure with the chemical water repellency of the organic compounds, a soil matrix can achieve high levels of hydrophobicity (McHale et al., 2005; McHale et al., 2007; Shirtcliffe et al., 2006; Bachmann and McHale, 2009).

Such high levels of hydrophobicity can have a number of deleterious effects on the natural landscape. Soil erosion during rainfall can become more pronounced (Terry and Shakesby, 1993), due to reduced water infiltration and hence an increase in surface runoff. The reduced infiltration results in drier soils that can also lead to an increase in wind erosion (DeBano, 2000). In addition there may be a corresponding reduction in the germination and growth of vegetation with the lower availability of water within the soil matrix.

Previous work has attempted to model the effects of water drop impacts on soils by using glass beads as a model soil (Hamlett et al., 2011, 2013; Ahn et al., 2013). Hamlett et al. (2013) investigated the behaviour of water drop impacts on bead packs (a layer of close packed, immobile beads with two layers of close packed, loose beads on top) which consisted of a single type of wettability (either hydrophobic or hydrophilic) throughout the entire depth of the bead pack. The authors investigated the pinning behaviour of the bead packs, where the droplet strikes the bead pack, spreads out, recoils and then cannot fully rebound from the surface and remains attached to the surface upon recoil, see Fig. 2.

This study expands on this and investigates the effect of layers of different hydrophobicity throughout the depth of the bead pack on both the drop impact behaviour and on the formation of liquid marbles (Aussillous and Quere, 2001; Nguyen et al., 2010). The effect on drop penetration and liquid marbling of mixing of hydrophobic and hydrophilic particles in powder beds was investigated by Nguyen et al. (2009), finding a reduction in drop penetration as the proportion of

hydrophobic particles increases. In this study the hydrophobic and hydrophilic particles are formed into discrete layers.

2. Experimental method

The experiment involved the creation of a number of bead packs, using glass beads between 140 µm and 400 µm (Worf Glaskugeln GmbH, Germany). Beads were ordered in a number of different colours in order to distinguish different layers within the bead packs. Before the bead packs could be created the beads were sieved and treated to make them either hydrophobic or hydrophilic. To sort the beads they were placed into small-scale sieves (Endecotts Ltd, UK) and an Endecotts Minor 200 sieve shaker (Endecotts Ltd, UK) to separate them into size categories. The categories used in this study are 140–160 µm, 160–180 µm, 180–200 µm, 250–300 µm and 400 µm, which correspond to fine and medium sized sandy soils (Soil Survey Division Staff., 1993).

Both hydrophobic and hydrophilic beads were needed for this study, and this required two separate processes. The first step was common to both types of beads and involved the beads being immersed in HCl (30 vol%) for 24 h, then rinsed thoroughly with deionised water (DI) until a strip of indicator paper showed that the DI water, after rinsing the beads, was neutral. Finally the beads were then placed in an oven at 80 °C for 3 h in order to dry the beads completely.

To make the hydrophobic beads, some of those previously cleaned with HCl were treated using Granger's Extreme Wash-In (Grangers, UK). A solution of Granger's in DI was prepared (5 vol%) and the beads were immersed in the solution for 1 hour. The beads were then dried in an oven at 80 °C for 3 h. Using a DSA 10 contact angle meter (Krüss, Germany) and analysed using DSA software (Krüss), the hydrophobised beads showed contact angles from 117° to 133°. The contact angle of each bead size was measured twice, showing no correlation between bead size and contact angle and a standard deviation of 5.60. A contact angle of 133° is comparable to a contact angle of 130° found by McHale et al on sand particles approximately 200 µm in size (McHale et al., 2005).

The hydrophilic beads were made by applying a titanium oxide coating to the surface of the beads. While glass is typically hydrophilic after being cleaned with HCl (Hamlett et al., 2013), the colour coating on the beads caused them to be hydrophobic. The beads were placed into a small dish and then into an Emitech K575X sputter coater (Quorum Technologies Ltd, UK). Titanium was sputtered onto the beads for 3 min at a current of 150 mA; the beads were then agitated and sputtered again to coat all sides of the beads. Next the titanium coated beads were placed into an ozone cleaner (BIO-FORCE Nanosciences, USA) for 20 min in order to produce an oxide layer on the surface of the beads. Water droplets placed onto the ozone treated beads immediately imbibed into the bead pack, as a result it was not possible to take contact angle measurements.

The bead packs consisted of three layers, a close packed base layer which was fixed in place and two loose layers on top of this. To produce the base layer, a mono layer of beads was fixed to a microscope slide using double sided tape. The fixed layer was then sputtered with Ti for 3 min at 150 mA and then gold (Au) for 3 min at 85 mA. If hydrophobic base layers were needed, they were treated with Granger's as above; hydrophilic base layers had a further layer of Ti sputter as above and then ozone treated as above to form an oxide layer. To form the

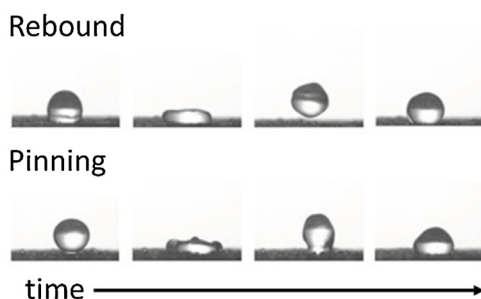


Fig. 2 – Images, taken from a high speed video recording, show the difference between rebound and pinning behaviour of a droplet impacting on a fixed, particulate surface.

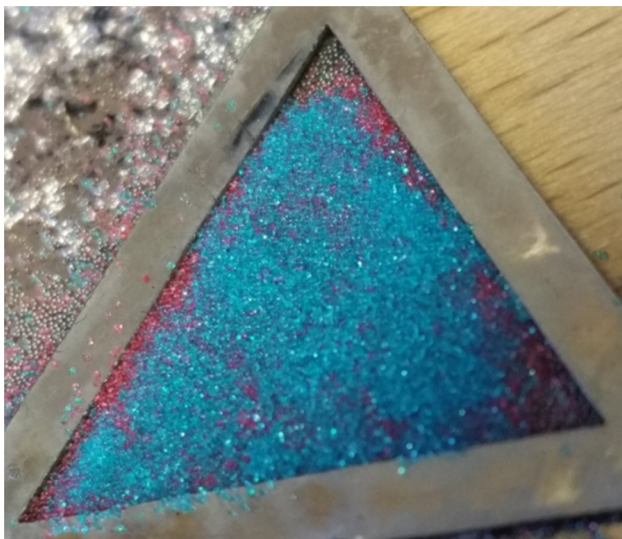


Fig. 3 – Image showing an example of a bead pack prior to drop impact experiment. Beads have been formed into layers of different colour, to investigate which layers the droplet is interacting with. (For interpretation of the references to colour in this figure legend, the reader is referred to the web version of this article.)

second layer, loose beads were placed on top of the base layer and agitated to try to form a single layer of particles. The third layer was then formed by placing loose beads on top again and agitated in order to try and form a single layer of beads. Care was taken to prevent the loose layers from mixing to try to form as close to a mono layer of beads and possible, see Fig. 3.

For the experimental work the bead packs were created with layers in different configurations of hydrophobic and hydrophilic, Fig. 4. The configurations ranged from a completely hydrophobic bead pack to a completely hydrophilic one with other configurations alternating hydrophobic and hydrophilic layers. For each bead pack, different coloured beads were used for the hydrophobic and hydrophilic layers in order to tell the layers apart during the drop impact measurements, to determine which layer the droplet is interacting with. The colours used in the diagrams in Fig. 4, and subsequent figures, denote the wettability of the bead and are not indicative of the physical colour of the bead.

The drop impacts were recorded at 5000 fps with a high speed camera, a Hotshot 512SC (NAC Image Technology, UK). A syringe was suspended at a known height above the bead pack and a single droplet of DI with a radius of 1.65 ± 0.02 mm (volume 0.019 ± 0.001 ml) dispensed so that it would fall directly

onto the beads. The high speed camera was used to record the impact event and a separate digital camera was used to take a still image of the aftermath of the impact. The height of the syringe was varied up to 250 mm in steps of approximately 10 mm to change the impact velocity of the water droplet. The impact for each bead back configuration was repeated twice for each drop height. The video footage was then analysed using ImageJ software (<http://imagej.nih.gov/ij/>).

3. Results and discussion

There were five different bead pack configurations used in this investigation, see Fig. 4, and for each configuration there were five bead sizes tested. This section will discuss the impact behaviour, transition velocities and liquid marbling for each configuration and for the bead sizes used.

Fig. 5 shows frame grabs from videos of the drop impacts. The frames depict a droplet falling at 0.93 ms^{-1} immediately prior to impacting the bead pack; followed by impact and spreading of the droplet and then bounce or pinning to the surface. All five bead pack configurations are shown for comparison.

Fig. 6 compares the droplet immediately after the impact has taken place and the droplet has reached equilibrium for the five different bead pack configurations with $180\text{--}200\mu\text{m}$ beads. Images are shown for increasing impact velocity, showing how the increase in velocity affects resulting droplet.

Table 1 shows the pinning and fragmentation velocities measured for all five bead packs at all bead sizes. The pinning velocity refers to the minimum velocity at which a transition from rebound to pinning was observed; and the fragmentation velocity refers to the minimum velocity at which a transition from pinning to fragmentation was observed. More detailed discussion is in the following sections.

3.1. Configuration 1 (hydrophobic (base layer)-hydrophobic-hydrophobic)

This bead pack consisted of purely hydrophobic particles. In the case of a hydrophobic top layer, the droplet shows clear liquid marbling behaviour, whereby the hydrophobic particles form a coating around the outside of the droplet. Column 1 in Fig. 5 shows frames from an impact video for an impact velocity of 0.93 ms^{-1} onto $180\text{--}200\mu\text{m}$ beads; after impact the droplet shows almost complete covering of beads to form a liquid marble. The liquid marble effect can be seen on all bead sizes and at all impact velocities; the degree of liquid marbling

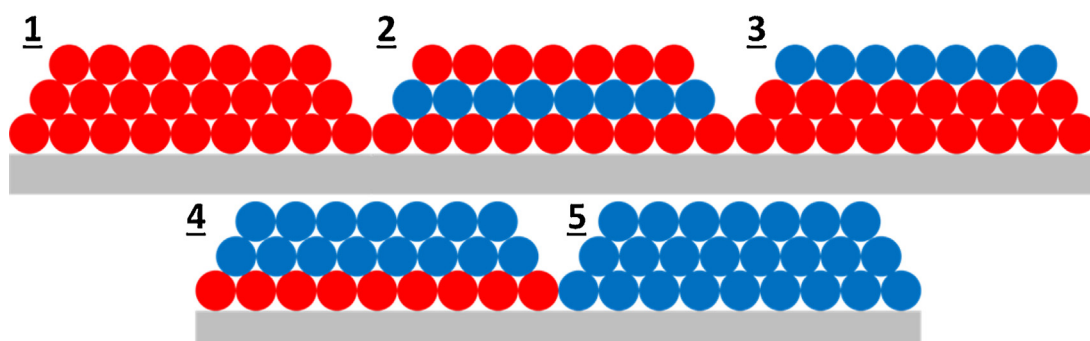


Fig. 4 – Idealised representations of the bead pack configurations, showing wettability of the layers of glass beads used in this study. Blue denotes hydrophilic beads and red denotes hydrophobic beads. (For interpretation of the references to colour in this figure legend, the reader is referred to the web version of this article.)

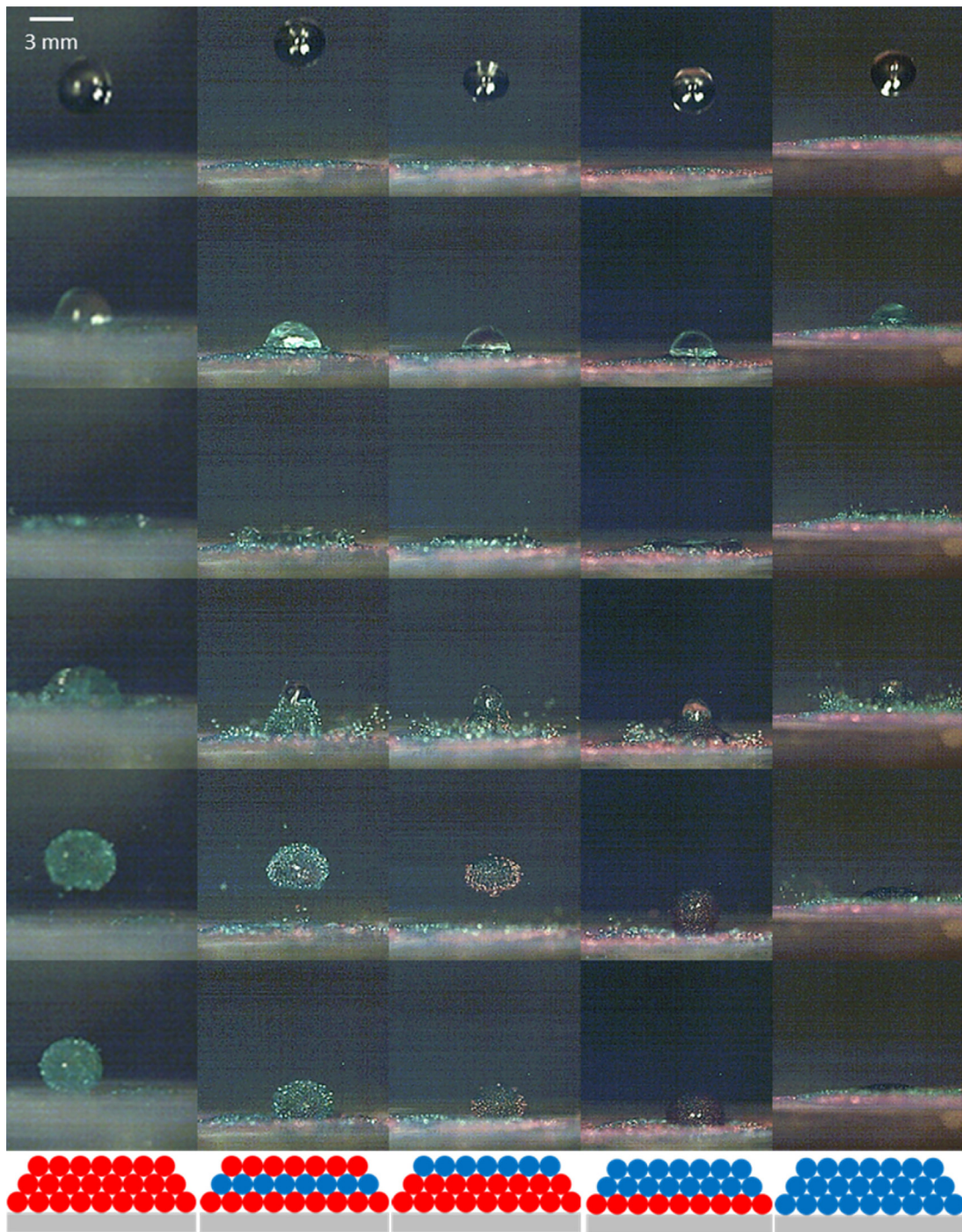


Fig. 5 – Comparative still images from video showing 0.93 ms^{-1} droplet impacting bead pack configurations 1–5 for 180–200 μm beads. Images show liquid marbling of hydrophobic beads, absorption of hydrophilic beads and wetting of wholly hydrophilic bead pack. Schematic of bead pack shown at the bottom of the image, indicating which layers are hydrophobic (red) or hydrophilic (blue). (For interpretation of the references to colour in this figure legend, the reader is referred to the web version of this article.)

and which bead pack layer contributes to the marble varies with bead size and impact velocity.

Row 1 in Fig. 6 shows the droplet after impact at four different impact velocities. The degree to which the beads coat the surface is seen to increase with impact velocity. By observing the colour of the beads coating the drop it can be seen that the majority are from the top layer, showing that the droplet mainly interacts with the top layer of the pack and not the lower layer.

When measuring the transition velocities there was no clear relationship between the bead size and the

velocity, Table 1. The 180–200 and 250–300 μm beads transition from bouncing to fragmentation with no pinning regime in-between. The 250–300 μm beads also showed the lowest fragmentation velocity. The other bead sizes showed similar pinning velocities, but the fragmentation velocities varied more. Of interest is that there was no measured pinning velocity for the 180–200 and 250–300 μm beads. This would require further investigate to explain, but may be attributable to the narrow gap between the pinning and fragmentation velocities resulting in the pinning transition not being observed.

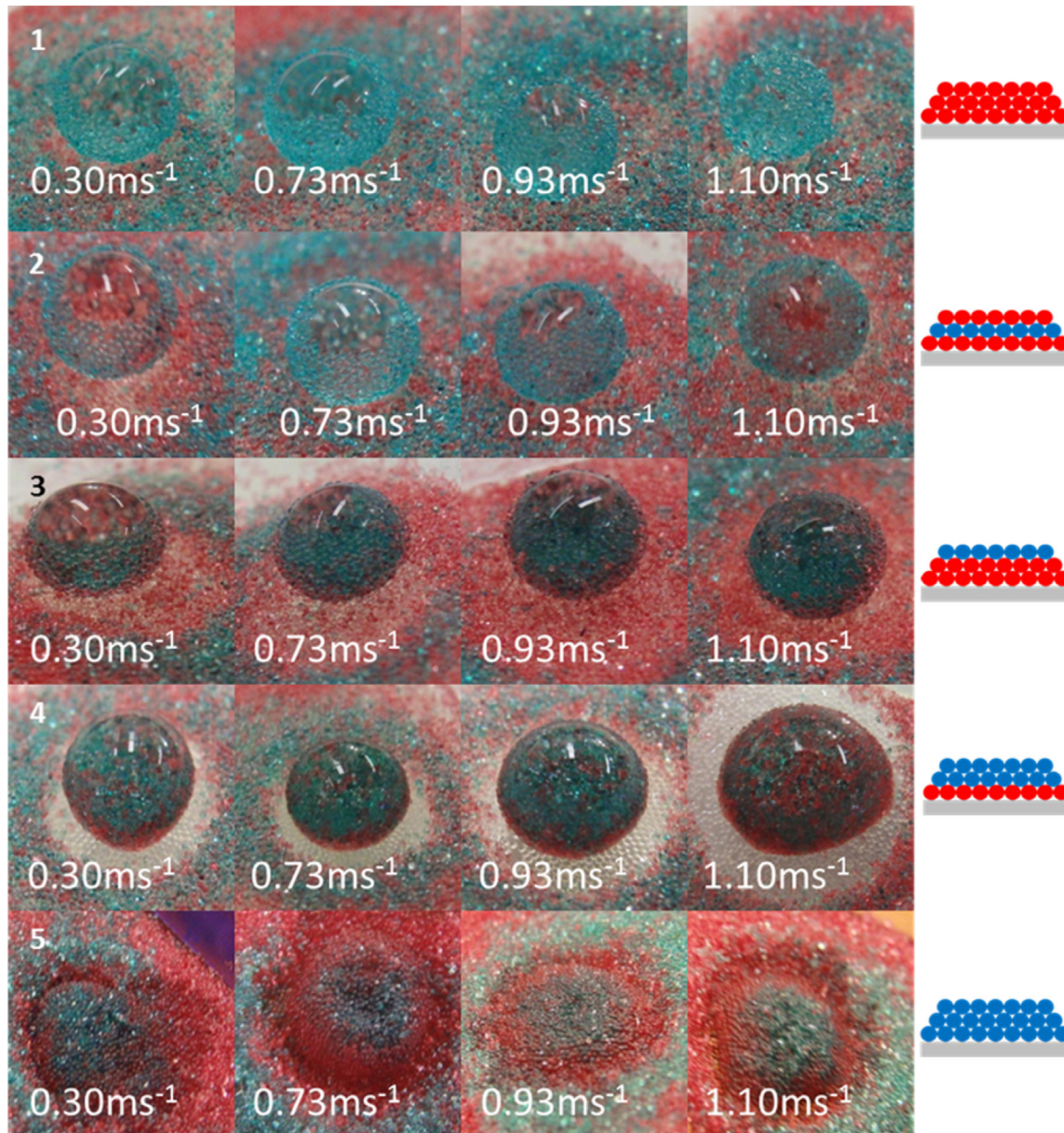


Fig. 6 – Images showing the droplet impact zones immediately after impact for bead pack configurations 1–5 and at different impact velocities. Schematic of bead pack shown on the right, indicating which layers are hydrophobic (red) or hydrophilic (blue). (For interpretation of the references to colour in this figure legend, the reader is referred to the web version of this article.)

3.2. Configuration 2 (hydrophobic-hydrophilic-hydrophobic)

This bead pack consisted of a hydrophilic layer sandwiched between two hydrophobic layers. Column 2 in Fig. 5 shows frames from an impact video for an impact velocity of 0.93 ms^{-1} onto $180\text{--}200\text{ }\mu\text{m}$ beads and row 2 in Fig. 6 shows the droplets after impact for $180\text{--}200\text{ }\mu\text{m}$ beads. Similar to the ‘all hydrophobic’ bead pack, the droplet forms a liquid marble using the hydrophobic beads on the top layer of the pack. There appears to be little interaction with the hydrophilic beads in the middle layer. By forming a liquid marble with the top layer, a barrier is formed around the droplet preventing the water from interacting with the hydrophilic particles.

There appears to some relationship between bead size and pinning velocity, Table 1, with an overall decrease in pinning velocity as bead size increases. Fragmentation velocity shows great variation, with no clear decrease overall.

3.3. Configuration 3 (hydrophobic-hydrophobic-hydrophilic)

Unlike the previous two bead pack configurations, this bead pack had a layer of hydrophilic beads forming the top layer. Column 3 in Fig. 5 shows frames from an impact video for an impact velocity of 0.93 ms^{-1} onto $180\text{--}200\text{ }\mu\text{m}$ beads and row 3 in Fig. 6 shows the droplets after impact for $180\text{--}200\text{ }\mu\text{m}$ beads. This bead pack configuration showed markedly different behaviour as the droplet impacts the bead pack. As the droplet interacts with the hydrophilic top layer, the beads are absorbed into the droplet. Some of the middle layer hydrophobic beads start to form a liquid marble round the outside of the droplet, but this effect is much less significant than with the hydrophobic top layer. Once the droplet comes to rest it forms a ball on top of the hydrophobic beads.

Based solely on this configuration there is no clear relationship between bead size and transition velocity, Table 1.

Table 1 – Pining and Fragmentation velocities for all bead hydrologies and sizes. Equivalent Weber numbers given in brackets. Schematic of bead pack shown at the top, indicating which layers are hydrophobic (red) or hydrophilic (blue). Error values relate to measurement errors in the determination of the velocities.

Pack #	D_b (μm)	v_p (ms^{-1})	v_f (ms^{-1})	v_p (ms^{-1})	v_f (ms^{-1})	v_p (ms^{-1})	v_f (ms^{-1})	v_p (ms^{-1})	v_f (ms^{-1})	v_p (ms^{-1})	v_f (ms^{-1})	v_p (ms^{-1})	v_f (ms^{-1})	v_p (ms^{-1})	v_f (ms^{-1})	
1	140–160	0.97 ± 0.14 (4.4)	1.18 ± 0.17 (6.5)	1.13 ± 0.16 (5.9)	1.35 ± 0.19 (8.5)	1.23 ± 0.17 (7.0)	1.39 ± 0.2 (9.0)	0.83 ± 0.12 (3.2)	—	—	—	1.02 ± 0.15 (4.8)	—	—	1.38 ± 0.2 (8.9)	—
	160–180	0.87 ± 0.11 (3.5)	1.01 ± 0.13 (4.7)	1.01 ± 0.13 (4.7)	1.08 ± 0.14 (5.4)	0.89 ± 0.11 (3.7)	1.33 ± 0.18 (8.2)	1.07 ± 0.14 (5.3)	—	—	—	1.06 ± 0.14 (5.2)	—	—	—	—
	180–200	—	—	1.18 ± 0.17 (6.5)	1.10 ± 0.16 (5.6)	1.34 ± 0.19 (8.3)	1.55 ± 0.10 (11.2)	1.73 ± 0.07 (13.9)	0.20 ± 0.03 (0.2)	—	—	0.20 ± 0.03 (0.2)	—	—	—	—
	250–300	—	—	0.98 ± 0.13 (4.5)	0.78 ± 0.10 (2.8)	1.11 ± 0.14 (5.7)	0.89 ± 0.11 (3.7)	1.47 ± 0.2 (10.0)	0.85 ± 0.11 (3.4)	—	—	0.98 ± 0.13 (4.5)	—	—	—	—
	400	0.84 ± 0.11 (3.3)	1.23 ± 0.16 (7.0)	0.87 ± 0.11 (3.5)	1.23 ± 0.16 (7.0)	0.73 ± 0.09 (2.5)	—	—	0.50 ± 0.06 (1.2)	—	—	0.75 ± 0.09 (2.6)	—	—	—	—



Pack #



However, compared to the bead packs with a hydrophobic top layer, the fragmentation velocity is higher. The reason for this may be the absorption of the hydrophilic beads into the droplet. The presence of the hydrophilic beads may help to hold the droplet together due to the attractive forces between the water and the beads. As a result, impact velocities that would normally fragment the droplet, fail to do so in this case; this may be due to capillary forces acting to hold the droplet together as the liquid infiltrates between the hydrophilic beads.

3.4. Configuration 4 (hydrophobic-hydrophilic-hydrophilic)

This bead pack has both the top and middle layer hydrophilic and the fixed base layer hydrophobic. Column 4 in Fig. 5 shows frames from an impact video for an impact velocity of 0.93 ms^{-1} onto $180\text{--}200 \mu\text{m}$ beads and row 4 in Fig. 6 shows the droplets after impact for $180\text{--}200 \mu\text{m}$ beads. The droplets show similar behaviour to the previous pack configurations, except with no liquid marble effect as there are no loose hydrophobic beads present. The droplet absorbs both the top and middle layers, due to them both comprising of hydrophilic beads; interacting with both the top and middle layers equally. A circular void can be seen where the beads have been removed, exposing the base layer below. The size of the circular void increases with impact velocity, due to the droplet spreading more upon impact at higher velocities. As the base layer is hydrophobic, once the droplet reaches equilibrium, it is not able to spread and so forms a ball on the surface with the hydrophilic beads contained within.

The most significant observation of this bead pack is the lack of fragmentation, Table 1. Within the range of impact velocities tested, the droplet did not transition to fragmentation upon impact. The effect seen in the previous bead pack, with just the top layer hydrophilic, appears to be enhanced with the middle layer also hydrophilic. The droplet is able to absorb a greater number of beads by interacting with both the top and middle layers, the beads then act to hold the droplet together and prevent fragmentation.

3.5. Configuration 5 (hydrophilic-hydrophilic-hydrophilic)

The final bead pack configuration consisted of a hydrophilic base layer and hydrophilic top and middle layers. Column 5 in Fig. 5 shows frames from an impact video for an impact velocity of 0.93 ms^{-1} onto $180\text{--}200 \mu\text{m}$ beads and row 5 in Fig. 6 shows the droplets after impact for $180\text{--}200 \mu\text{m}$ beads. Due to the absence of hydrophobic beads present in the bead pack, there is no liquid marble behaviour or ball-like equilibrium droplet. The droplet spreads upon impact and recedes due to surface tension; at lower impact velocities the droplet bounces slightly. Once the droplet has come to rest it leaves a small mound of beads at the impact site, while the water wets into the bead pack.

Typically the pinning transition happens at lower velocities compared to the previous bead pack configurations, Table 1. For all but the $140\text{--}160 \mu\text{m}$ beads, the droplet failed to fragment in the range of velocities tested.

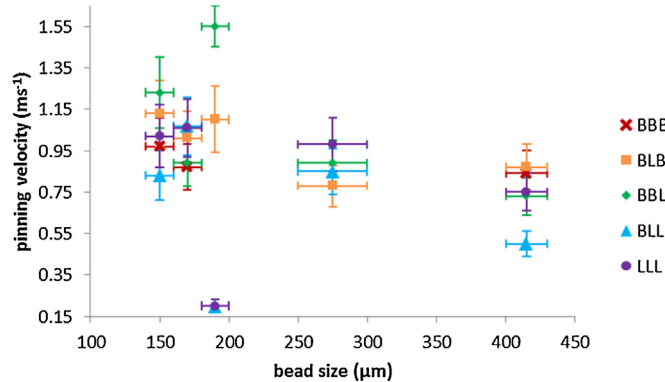


Fig. 7 – A graph showing the pinning velocities of the bead pack against bead size. Legend describes base layer to top layer and whether the layer is hydrophobic (B) or hydrophilic (L). Error in bead size due to difference in sieve sizes, velocity error due to measurement errors.

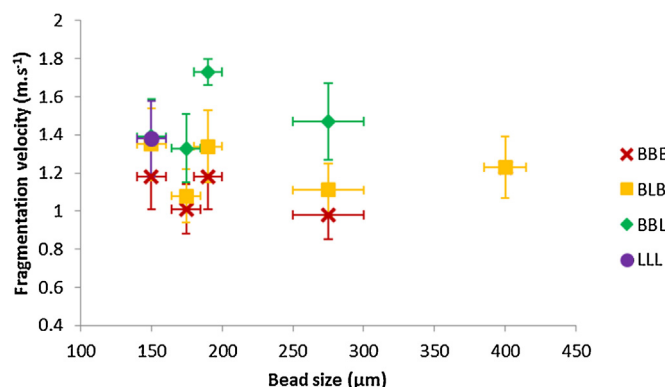


Fig. 8 – A graph showing the fragmentation velocities of the bead pack against bead size. Legend describes base layer to top layer and whether the layer is hydrophobic (B) or hydrophilic (L). Error in bead size due to difference in sieve sizes, velocity error due to measurement errors.

3.6. Pinning velocities

Fig. 7 compares the pinning velocities for all the bead pack configurations and bead sizes. By looking at the data set as a whole, there appears to be a general decrease in pinning velocity as the bead size increases. As in each case the impact results in the beads combining with the droplet, either through the liquid marble effect or absorption of hydrophilic beads; as the number of beads combined with the droplet increases the kinetic energy required to de-pin from the surface would increase, with the larger beads providing more mass and therefore causing the droplet to pin at a lower impact velocity.

The observed pinning velocities for the BLL and LLL cases on the 180–200 μm are significantly lower than all the other trials. While this may be due to imperfect bead packing, further investigation is needed to understand why this is the case.

3.7. Fragmentation velocities

Fig. 8 shows that fragmentation velocities for all the bead pack configurations and bead sizes. Unlike the pinning velocities, there is no clear trend between the particle size and the fragmentation velocity. This is consistent with the work of Hamlett et al. (2013) and also work by Reyssat et al. (2006) investigating ideal superhydrophobic surfaces. There is some evidence that hydrophilic top layers help to prevent droplet fragmentations. Configuration 4 shows no fragmentation at all and configuration 5 only shows fragmentation at the smallest bead size.

4. Conclusions

This work investigated the impact behaviour of water droplets on bead packs; consisting of sub-millimetre sized beads with varying configurations of hydrophobic and hydrophilic beads. This was carried out in order to gain a better understanding of the granular systems (e.g. soils or industrial materials) of mixed wettability under water drop impacts (e.g. rainfall, irrigation). By colour coding the layers of the bead pack it was possible to distinguish which layers the droplets had interacted with during the impact event.

In the case of bead packs with a hydrophobic top layer, the droplet would mostly interact with only the top layer, Fig. 9a. A liquid marble was formed as the beads coated the droplet, forming a solid barrier preventing the droplet from interacting with the lower layers. In the case of bead packs with hydrophilic middle layers, this prevented the droplet from wetting the middle layer and instead the liquid marble sat on top of the hydrophilic beads, Fig. 9b. Higher impact velocities resulted in a greater degree of liquid marbling, as the droplet would spread out more and gather up more of the hydrophobic beads, but also resulted in more interaction with the middle layer of the pack.

In the case of a hydrophilic top layer, the droplet was seen to absorb the hydrophilic beads. In a wholly hydrophilic bead pack this resulted in the droplet gathering together the beads to form a small mound where the impact took place; the droplet would then wet into the bead pack, Fig. 9e. If a loose hydrophobic layer was present then the droplet would start to form a liquid marble. The hydrophobic beads would form a

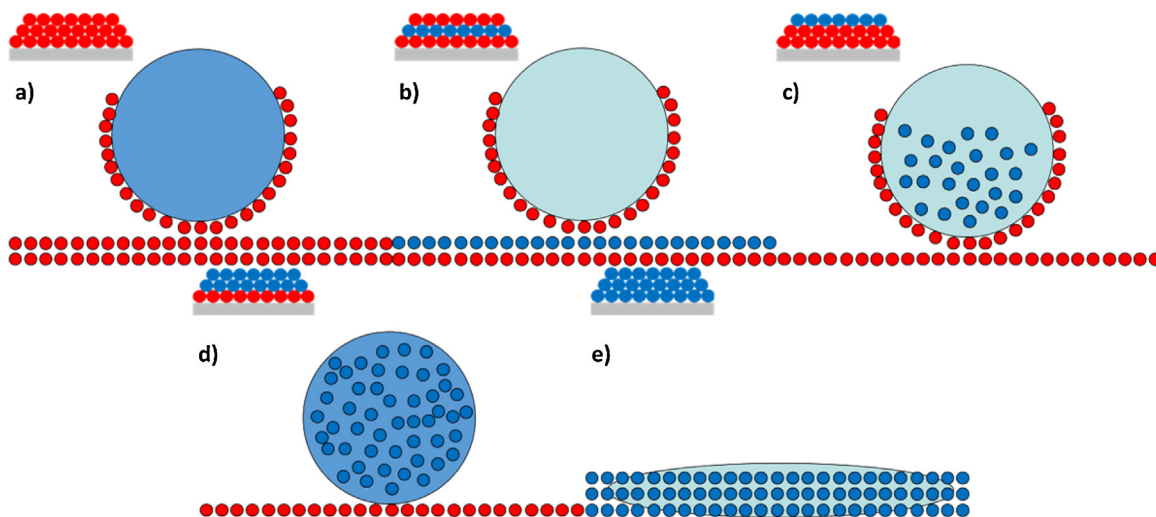


Fig. 9 – Diagram showing bead behaviour after droplet impact for each bead pack configuration. Schematic of bead pack shown at the top, indicating which layers are hydrophobic (red) or hydrophilic (blue). (For interpretation of the references to colour in this figure legend, the reader is referred to the web version of this article.)

coating around the outside of the droplet with the hydrophilic beads within the droplet, Fig. 9c. With a hydrophobic fixed base layer; the droplet would absorb the hydrophilic beads and then form a ball on top of the base layer, unable to wet the hydrophobic beads, Fig. 9d. Future work will expand on this with a full mathematical model.

Measurements of pinning velocities showed a general decrease in velocity as the size of the beads within the pack increased. The fragmentations velocities measured showed that the presence of hydrophilic beads within the bead pack helped to prevent the droplet from fragmenting upon impact; with the droplet failing to fragment in the velocity range investigated for the wholly hydrophilic and the hydrophilic top and middle layer bead packs.

In the context of the hydrological behaviour of soils or other granular materials; these results suggest that while a hydrophobic particle top layer can increase splash erosion due to liquid marbling (Hamlett et al., 2013), this effect will not penetrate into the matrix below for any given droplet. Hydrophobic particles just below the surface, however, may result multiple layers of the matrix eroding simultaneously. These differences in particle-scale behaviour could, for example, lead to distinct differences in splash erosion on hillslopes or on ridges in ploughed agricultural land where wind erosion processes may lead to a layered arrangement of soil particles with different wettabilities. Greater understanding of the interaction of rain droplets with soils will allow for targeted intervention to overcome the effects of erosion and reduced water infiltration. This will have benefits for forestation and agriculture, by helping to maintain the growth of vegetation.

This study shows a number of interesting effects when the wettability of the bead pack is altered. Future work will focus on building a model to explain the observed phenomenon; to relate the bead size, wettability and the pinning and fragmentation velocities of the bead packs.

Acknowledgements

The authors would like to thank the UK Engineering and Physical Sciences Research Council (EPSRC) for their support

and funding under grants EP/H000704/1, EP/H000747/1 and EP/E063489/1.

References

- Ahn, S., Doerr, S.H., Douglas, P., Bryant, R., Hamlett, C.A.E., McHale, G., Newton, M.I., Shirtcliffe, N.J., 2013. Effects of hydrophobicity on splash erosion of model soil particles by a single water drop impact. *Earth Processes Landforms* 38, 1225–1233.
- Atanassova, I., Doerr, S.H., 2010. Organic compounds of different extractability in total solvent extracts from soils of contrasting water repellency. *Eur. J. Soil Sci.* 61, 298–313.
- Aussillous, P., Quere, D., 2001. Liquid marbles. *Nature* 411, 924–927.
- Bachmann, J., McHale, G., 2009. Superhydrophobic surface: a model approach to predict contact angle and surface energy of soil particles. *Eur. J. Soil Sci.* 60, 420–430.
- Cassie, A.B.D., Baxter, S., 1944. Wettability of porous surfaces. *Trans. Faraday Soc.* 40, 546–551.
- DeBano, L.F., 2000. Water repellency in soils: a historical overview. *J. Hydrol.* 231–232, 4–32.
- Doerr, S.H., Shakesby, R.A., Walsh, R.P.D., 2000. Soil water repellency, its characteristics, causes and hydro-geomorphological consequences. *Earth Sci. Rev.* 51, 33–65.
- Ellerbrock, R.H., Gerke, H.H., Bachmann, J., Goebel, M., 2005. Composition of organic matter fractions for explaining wettability of three forest soils. *Soil Sci. Soc. Am. J.* 69, 57–66.
- Hamlett, C.A.E., Shirtcliffe, N.J., McHale, G., Ahn, S., Bryant, R., Doerr, S.H., Newton, M.I., 2011. Effect of particle size on droplet infiltration into hydrophobic porous media as a model of water repellent soil. *Environ. Sci. Technol.* 45, 9666–9670.
- Hamlett, C.A.E., Atherton, S., Shirtcliffe, N.J., McHale, G., Ahn, S., Bryant, R., Doerr, S.H., Newton, M.I., 2013. Transitions of water-drop impact behaviour on hydrophobic and hydrophilic particles. *Eur. J. Soil Sci.* 64, 324–333.
- McHale, G., Newton, M.I., Shirtcliffe, N.J., 2005. Water-repellent soil and its relationship to granularity, surface roughness and hydrophobicity: a materials science view. *Eur. J. Soil Sci.* 56 (2005), 445–452.
- McHale, G., Shirtcliffe, N.J., Newton, M.I., Pyatt, F.B., 2007. Implications of ideas on super-hydrophobicity on water repellent soil. *Hydrol. Processes* 21, 2229–2238.
- Nguyen, T., Shen, W., Hapgood, K., 2009. Drop penetration time in heterogeneous powder beds. *Chem. Eng. Sci.* 64, 5210–5221.

- Nguyen, T., Hapgood, K., Shen, W., 2010. Observation of the liquid marble morphology using confocal microscopy. *Chem. Eng. J.* 162, 396–405.
- Reyssat, M., Pepin, A., Marty, F., Chen, Y., Quere, D., 2006. Bouncing transitions on microtextured materials. *Europhys. Lett.* 74, 306–312.
- Shirtcliffe, N.J., McHale, G., Newton, M.I., Pyatt, F.B., 2006. Critical conditions for the wetting of soils. *Appl. Phys. Lett.* 89, 094101.
- Shirtcliffe, N.J., McHale, G., Atherton, S., Newton, M.I., 2010. An introduction to superhydrophobicity. *Adv. Colloid Interface Sci.* 161, 124–138.
- Soil Survey Division Staff, 1993. *Soil survey manual*. In: Soil Conservation Service. U.S. Department of Agriculture Handbook, pp. 18.
- Terry, J.P., Shakesby, R.A., 1993. Soil water repellency effects on rainsplash: simulated rainfall and photographic evidence. *Earth Surf. Processes Landforms* 18, 519–525.
- Wenzel, R.N., 1936. Resistance of solid surfaces to wetting by water. *Ind. Eng. Chem.* 28, 988–994.
- Zisman, W.A., 1964. Contact angle, wettability, and adhesion. *Am. Chem. Soc.* 43, 1–51.